

Investigation of the Interaction Between Human Serum Albumin and Two Drugs as Binary and Ternary Systems

Nooshin Abdollahpour¹ · Vahid Soheili² · Mohammad Reza Saberi³ · Jamshidkhan Chamani⁴

Published online: 2 September 2015
© Springer International Publishing Switzerland 2015

Abstract

Background and Objectives Human serum albumin (HSA) is the most frequent protein in blood plasma. Albumin transports various compounds, preserves osmotic pressure, and buffers pH. A unique feature of albumin is its ability to bind drugs and other bioactive molecules. However, it is important to consider binary and ternary systems of two pharmaceuticals to estimate the effect of the first drug on the second one and physicochemical properties.

Methods Different techniques including time-resolved, second-derivative and anisotropy fluorescence spectroscopy, resonance light scattering (RLS), critical induced aggregation concentration (C_{CIAC}), particle size, zeta potential and stability analysis were employed in this

assessment to elucidate the binding behavior of Amlodipine and Aspirin to HSA. Moreover, isothermal titration calorimetric techniques were performed and the QSAR properties were applied to analyze the hydration energy and $\log P$. Multiple sequence alignments were also used to predict the structure and biological characteristics of the HSA binding site.

Result Time-resolved fluorescence spectroscopy showed interaction of both drugs to HSA based on a static quenching mechanism. Subsequently, second-derivative fluorescence spectroscopy presented different values of parameter H in binary and ternary systems, which were suggested that tryptophan was in a more polar environment in the ternary system than in a binary system. Moreover, the polydispersity index and results from mean number measurements revealed that the presence of the second drug caused a decrease in the stability of systems and increased the heterogeneity of complex. It is also, observed that the gradual addition of HSA has led to a marked increase in fluorescence anisotropy (r) of Amlodipine and Aspirin which can be suggested that the drugs were located in a restricted environment of the protein as confirmed by Red Edge Excitation Shift (REES) studies. The isothermal titration calorimetric technique demonstrated that the interaction of the drugs with HSA was an enthalpically-driven process.

Conclusions The present experiment showed that the binding of Amlodipine and Aspirin to HSA induced a conformational change of HSA. It was also identified that the protein binding of the first drug could be affected by the second drug. Such results can be of great use for understanding the pharmacokinetic and pharmacodynamic mechanisms of drugs.

✉ Vahid Soheili
Soheiliv881@mums.ac.ir

✉ Jamshidkhan Chamani
chamani@ibb.ut.ac.ir

¹ Department of Biology, Faculty of Sciences, Young Researchers and Elite Club, Islamic Azad University-Mashhad Branch, Mashhad, Iran

² Department of Drug Control, School of Pharmacy, Mashhad University of Medical Sciences, Mashhad, Iran

³ Department of Medicinal Chemistry, School of Pharmacy, Mashhad University of Medical Sciences, Mashhad, Iran

⁴ Department of Biology, Faculty of Sciences, Mashhad Branch, Islamic Azad University, Mashhad, Iran

Key points

The interaction of Amlodipine and Aspirin with HSA was investigated by different techniques.

A comparison of the results of fluorescence and other spectral analyses was also performed in order to assess the localization of the drug in the model system.

The present experiment showed that the binding of Amlodipine and Aspirin to HSA induced a conformational change of HSA.

We concluded that the presence of Aspirin in (HSA–Aspirin)–Amlodipine system can cause a reduction in affinity of Amlodipine to binding in HSA.

1 Introduction

Human serum albumin (HSA) is an extensively studied plasma protein. A unique feature of albumin is its ability to bind drugs and other bioactive molecules [1]. HSA is characterized by high cysteine content, stabilizing a series of nine loops and a Trp residue. Despite the size and complexities of HSA, there is only a single Trp residue (Trp 214) in domain II, which facilitates the study of the protein from a spectroscopic point of view. This single Trp is responsible for the intrinsic protein fluorescence. Serum albumin effectively increases the solubility of hydrophobic drugs in plasma and modulates their delivery to cells both *in vivo* and *in vitro* [2]. More ever, unfolding of HSA has been thoroughly studied by several biophysical techniques and at varying denaturing conditions.

It is generally accepted that the distribution, metabolism, excretion and toxicity of ligands are correlated with their affinities toward the protein, especially serum albumin. To clearly understand these factors, the characterization of the binding process by estimating the binding affinity and binding site is imperative and has a fundamental importance in the biological system [3].

Amlodipine is widely used for the treatment of hypertension as well as stable and variant angina. It is more effective than β -blockers when it comes to treating variant angina because it prevents and reverses the coronary spasms resulting in an increased blood flow and myocardial vasculature smooth muscle cell proliferation. This, in turn, prevents a progressive narrowing of the arteries [4].

Acetyl salicylic acid or Aspirin is a non-steroidal anti-inflammatory drug [5]. Today, Aspirin is one of the most

widely used medications in the world, with an estimated 40,000 metric tons consumed each year [6]. It has also been established that low doses of Aspirin may be given immediately after a heart attack to reduce the risk of another heart attack or prevent the death of cardiac tissue [7].

In general, protein stability depends on internal factors, such as hydrogen bonding and covalent linkages, the environment, the binding of ligands and interactions with biological surfaces [8]. For this reason, a combined experimental investigation is often performed and optical methods are supported by RLS, zeta potential and PDI. Such techniques render it possible to focus on different aspects of protein–ligand systems and give more information on ligand binding, protein conformation, and change distribution. Like most biophysical techniques, fluorescence spectroscopic studies can be carried out at many levels ranging from simple measurements of steady-state emission intensity to quite sophisticated time-resolved studies. The information content raises considerably as different fluorescence observables are time-resolved and combined in universal analyses of the interest phenomena. These measurements can be applied to get hydrodynamic information about macromolecules and macromolecule complexes.

Since the tryptophan residues intrinsic to proteins and bound covalently ligand molecules almost always exhibit local rotational motion in addition to depolarization through global Brownian tumbling of the macromolecule, it is wise to measure the time-resolved fluorescence anisotropy as well as that observed in the steady-state mode [9]. The present paper deals with the mechanism of binding of Amlodipine and Aspirin as a ligand with HSA by time-resolved fluorescence measurements. Anisotropy measurements reveal that the average angular displacement of the fluorophore that alters the rotational correlation time will also alter the anisotropy. For biomolecules, the anisotropy decreases due to both rotational diffusion and internal flexibility. Also, fluorescence quenching can be studied most excellent by time-resolved techniques, which can be divided into static and dynamic processes. Conformational changes in proteins often result in changes in intensity decays due to altered interactions with nearby groups. Time-resolved decays can sometimes be interpreted as the location of the tryptophan residues in the protein, and the interactions of these residues with nearby amino acid residues [9].

This study highlights for the first time how binding properties can change for HSA. Primarily, four types of forces take part in the protein–drug interaction such as electrostatic forces, hydrophobic forces, van der Waals interactions and hydrogen bonding. Signs and magnitudes of the thermodynamic parameters determine the nature of

forces actually participating in the protein-drug interaction. The analysis of thermodynamic parameters, combined with the study of physicochemical properties of the phenomena, provides an understanding of how the two molecules interact and what thermodynamic processes control the conformational rearrangements of molecules [10].

The inter-relationships between members of a protein family are better illustrated by multiple alignments, e.g., the fortuitous absence of a mutation at that particular site, but if the same residue is found in five or ten proteins in a family, it can be suggested that the residue may play a key functional role. This alignment shows that some residues are absolutely conserved; certain positions are occupied by very similar amino acid residues and other more variable ones [11].

In this study, we found protein sequences belonging to the serum albumin family with identical length, through UniProt identifiers. In order to obtain multiple alignments, we marked three protein sequences using the checkboxes found in BLAST results. The hit value was set to '1000' to limit the number of returned alignments. Also, we selected the align tab of the toolbar to perform an alignment with the ClustalW program. Subsequently, another protein was added and the results were saved. This was repeated until we selected 20 albumin proteins belonging to different animals. Finally, we could observe some amino acid residues that were conserved in these proteins.

To analyze and predict the structure and biological characteristics of binding sites of HSA, the Expert Protein Analysis System (ExPASy) and other bioinformatics software were used [12]. ProtScale, the analysis software that is available through ExPASy, renders possible the computation and representation of the profile produced by any amino acid scale on a selected protein [13]. So, we used two corresponding methods in this work, i.e., hydrophobicity and polarity, which are represented by ProtScale.

The literature comprises numerous articles on the determination of ligand interactions with proteins but there have been no reports on the binding affinity and binding mechanism of a ternary system to a plasma protein (especially serum albumin). This could supply salient insight into the mechanism of interaction of Amlodipine and Aspirin with HSA and other physiologically important proteins. We have previously reported spectroscopic studies to characterize the interactions of some drugs with HSA [14]. The aim of this study has been to elucidate the binding behavior of Amlodipine to HSA, and also to determine other binding and physicochemical properties by the combined use of spectroscopic techniques. A comparison of the results of fluorescence and other spectral analyses was also performed in order to assess the localization of the drug in the model system.

2 Experimental Section

2.1 Apparatus

All fluorescence measurements were carried out on an F-2500 spectrophotometer (Hitachi, Japan) equipped with 1.0-cm quartz cells and a thermostat bath with a xenon lamp. The excitation wavelengths were set to 280 and 295 nm, and the excitation and emission slit widths were 5 nm. The scan speed was 1200 nm/min, and the PMT (Photo Multiplier Tube) voltage was 700 V. Fluorescence intensities were corrected for inner filter and dilution effects before analysis of the binding and quenching data. The RLS spectra were recorded with an F-2500 fluorescence spectrophotometer (Hitachi, Japan) by simultaneously scanning the excitation and emission spectra from 280 to 600 nm with $\Delta\lambda = 0$ nm and a slit width of 5.0 nm. This rendered it possible to investigate the aggregation of small molecules and the long-range assembly of drugs on biological templates. The other scanning parameters were identical to those of the fluorescence quenching spectra. All pH measurements were made with a Metrohm digital pH-meter (Metrohm, Germany). In ITC experiment, the Origin[®] scientific plotting software (version 6) was used to analyze calorimetric data. The multiple sequence alignments were generated by the ClustalW (version 3 at EBI) site for sequence analysis through the BLAST engine [11, 15]. We designed multiple alignments so that three sequences of similar proteins were selected in the first step and the multiple alignments were carried out with ClustalW. In the next step, the number of sequences was increased to 4 and the procedure was repeated until the number of sequences reached 20. The ProtScale software and site [through Expert Protein Analysis System (ExPASy)] was utilized to predict and analyze structures and functions of the proteins [12]. The hydration energy and log P are some of the properties that could be estimated using QSAR properties from the HyperChem software. The hydration energy (for peptides and similar systems) was determined using the method parameterized by Scheraga et al. [16], based on an approximate surface area calculation. Log P (the log of the octanol–water partition coefficient), a hydrophobicity indicator, was also utilized by an atom fragment method developed by Ghose, Pritchett and Crippen [17].

2.1.1 Measurement of the Physicochemical Properties of the Drug/Protein Complexes

The average particle size, polydispersity index (PI) and zeta potential at different concentrations were characterized using a zeta-sizer Nano ZS90 (Malvern,

Worcestershire, UK) at a temperature of 25 °C. The zeta potential characterizes the surface charge of particles, which is an indicator of the long-term stability. Samples were diluted with water (adjusted to pH 7.4) to a suitable concentration before the analysis of the size distribution. The PI is an indication of the particle size distribution.

2.2 Reagents

HSA (fatty acid free, 90 %), Aspirin and Amlodipine were purchased from Sigma Chemical Co. (St. Louis, Mo. USA). The protein was dissolved to 50-mM in phosphate buffer of pH 7.4 and the stock solution was kept in the dark at 4 °C. All starting materials were analytical reagent grade and double-distilled water was used for all the measurements. Aspirin and Amlodipine were dissolved in the buffer and diluted to 0.05 and 0.002 mM, respectively, corresponding to low usage dose concentrations, with the solution consisting of 50-mM in potassium phosphate at pH 7.4. In measurements for each data point, 10 μ l of the drug solution was added to 2 ml of the HSA solution (4.25×10^{-6} mM). The interaction time was investigated and the results showed that 3 min was enough for the stabilization. The fluorescence spectra were then measured (the excitation wavelengths were 280 and 295 nm and the emission wavelengths were 290–600 nm). The PI and zeta potential measurements of HSA–Amlodipine and HSA–Aspirin were recorded and spectral scanning curves were obtained under the same conditions.

3 Results and Discussion

3.1 Fluorescence Quenching

Fluorescence spectroscopy can be applied to a wide range of problems in the chemical and biological sciences. These measurements can provide information on a wide range of molecular processes, including the interactions of solvent molecules with fluorophores, rotational diffusion of biomolecules, and distances between sites on biomolecules, conformational changes, and binding interactions.

For collisional quenching, the decrease in intensity is described by the well-known Stern–Volmer equation (Eq. 1):

$$F_0/F_1 = 1 + k_q \tau_0 [Q] = 1 + K_{sv} [Q] \quad (1)$$

In this equation F_0 and F in dynamic quenching are the fluorescence intensities in the absence and presence of quencher, respectively; k_q is the bimolecular quenching constant given by $K_{sv} = k_q \tau_0$. τ_0 is the unquenched lifetime, and $[Q]$ is the quencher concentration. The Stern–Volmer quenching constant (K_{sv}) indicates the sensitivity of the fluorophore to a quencher. A fluorophore buried in a macromolecule is usually

inaccessible to water-soluble quenchers, causing the value of K_{sv} to be low. Larger values of K_{sv} are found if the fluorophore is free in solution or on the surface of a biomolecule [9].

Intrinsic protein fluorescence originates from the aromatic amino acids Trp, Tyr and Phe. In proteins, the dominant fluorophore is the indole group of Trp. Indole absorbs near 280 nm, and emits near 340 nm. The emission spectrum of indole is highly sensitive to solvent polarity. The emission of indole may be blue-shifted if the group is buried within a native protein (N), and its emission may shift to longer wavelengths (red shift) when the protein is unfolded (U). The emission of Trp is highly sensitive to its local environment, and is thus often used as a reporter group for protein conformational changes [9].

The quenching of HSA fluorescence was performed at pH 7.4 in the presence of Aspirin at various concentrations of Amlodipine, and the results are shown in Fig. 1a. As can be seen, the fluorescence intensity of HSA gradually decreased with an increasing Amlodipine concentration. Addition of Amlodipine in the presence of Aspirin caused a noticeable decrease in HSA fluorescence intensity. The maximum emission wavelength showed a blue shift and corresponded to changes in the micro-environment of the protein. Quenching data are usually presented as plots of

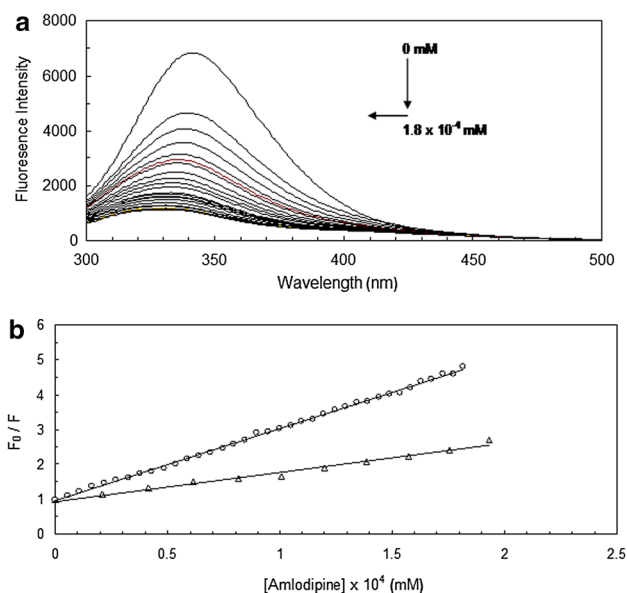


Fig. 1 **a** The quenching of intrinsic HSA fluorescence by Amlodipine in the ternary system. Conditions: $T = 298$ K, $\text{pH} = 7.4$, $\lambda_{\text{ex}} = 280$ nm. The concentration of HSA was 4.5×10^{-3} mM and those of Amlodipine and Aspirin were increased from 1.8×10^{-4} mM (for the sake of clarity, the blue-shifts are shown with *arrows*). **b** A comparison of the Stern–Volmer plots for the binary HSA–Amlodipine (*open circle*), ternary (HSA–Aspirin)–Amlodipine (*open triangle*) systems. Conditions: $T = 298$ K, $\text{pH} = 7.4$, $\lambda_{\text{ex}} = 280$ nm, $[\text{HSA}] = 4.5 \times 10^{-3}$ mM, $[\text{Amlodipine}] = 0$ – 1.8×10^{-4} mM, $[\text{Aspirin}] = 0$ to 8.5×10^{-3} mM

F_0/F versus $[Q]$ since F_0/F is expected to be linearly dependent upon the concentration of the quencher. A plot of F_0/F versus $[Q]$ yields an intercept of 1 on the y-axis and a slope equal to K_D . It is useful to note that K_D^{-1} is the quencher concentration at which $F_0/F = 2$ or at which 50 % of the intensity is quenched. A linear Stern–Volmer plot is generally indicative of a single class of fluorophores, all equally accessible to the quencher. As shown in Fig. 1b, there was one type of binding site for Amlodipine in the binary and ternary systems of (HSA–Aspirin)–Amlodipine.

On the graphs representing the Stern–Volmer equation (Fig. 1b), the slope of the curves decreased, in comparison with the binary system, with a gradual addition of Amlodipine to the HSA–Aspirin complex. This effect might suggest a diminution of the movement of molecules within their binding sites probably related to the presence of a large number of molecules of both ligands in subdomains IIA and IIIA [18]. Moreover, this indicates that the fluorophore of the protein was placed in a more hydrophobic micro-environment in the presence of Amlodipine and Aspirin [19].

The different mechanisms of quenching are usually classified as either dynamic or static. Dynamic and static quenching can be distinguished by their differing dependence on temperature, viscosity and also lifetime. Since a higher temperature results in larger diffusion coefficients, the dynamic quenching constants are expected to increase with increasing temperature. A higher temperature is likely to give rise to a decreased stability of the complexes, and thus to lower values of the static quenching constants [20]. Accordingly, the Stern–Volmer equation was applied to

determine K_{SV} by linear regression of a plot of F_0/F against $[Q]$.

Table 1 summarizes the calculated K_{SV} at different temperatures. It can be seen that K_{SV} is inversely correlated with the temperature, which suggests that the fluorescence quenching process may be mainly controlled by a static quenching mechanism rather than a dynamic one [21]. These results indicate that the fluorescence quenching was caused by a specific interaction, and that the quenching mainly arose from complex formation [20]. This result further confirmed that the quenching was mainly a static process. The results also show that the Stern–Volmer dynamic quenching constant K_{SV} was inversely correlated with the temperature, indicating that the probable quenching mechanism of fluorescence of HSA by Amlodipine was not initiated by dynamic collision but by compound formation [22].

3.2 Measurement of Thermodynamic Parameters

The molecular forces contributing to protein interactions with ligands may be van der Waals forces; hydrogen bonding; electrostatic or hydrophobic interactions. The thermodynamic parameters, the enthalpy (ΔH^0) and entropy (ΔS^0) of the binding reaction, are important to confirm the force of interactions of ligands with biomolecules. Therefore, the temperature dependence of the binding constants was studied at different temperatures (298, 308, 318 K). If the enthalpy changes do not vary significantly over the investigated temperature range, then its

Table 1 Stern–Volmer quenching constants of the different systems at various temperatures and relative thermodynamic parameters at pH7.4

System	T (K)	K_{SV} (L mol ⁻¹)	ΔG^0 (kJ mol ⁻¹)	ΔH^0 (kJ mol ⁻¹)	ΔS^0 (J mol ⁻¹ K ⁻¹)
HSA–Aspirin	298	$(1.03 \pm 0.01) \times 10^6$	-34.30		
	308	$(9.91 \pm 0.01) \times 10^5$	-35.35	-17.43	58.18
	318	$(9.79 \pm 0.01) \times 10^5$	-36.47		
(HSA–Amlodipine)–Aspirin	298	$K_{SV1} = (3.36 \pm 0.03) \times 10^5$	-31.54		
		$K_{SV2} = (6.14 \pm 0.03) \times 10^5$	-33.02		
	308	$K_{SV1} = (3.21 \pm 0.03) \times 10^5$	-32.47	$\Delta H_1^0 = 11.27$	$\Delta S_1^0 = 142.01$
		$K_{SV2} = (3.05 \pm 0.03) \times 10^5$	-32.34	$\Delta H_2^0 = -22.19$	$\Delta S_2^0 = 32.95$
	318	$K_{SV1} = (3.11 \pm 0.03) \times 10^5$	-33.44		
		$K_{SV2} = (2.95 \pm 0.03) \times 10^5$	-33.31		
HSA–Amlodipine	298	$(2.07 \pm 0.02) \times 10^7$	-41.74		
	308	$(1.88 \pm 0.03) \times 10^7$	-42.89	-21.34	69.97
	318	$(1.63 \pm 0.02) \times 10^7$	-43.90		
(HSA–Aspirin)–Amlodipine	298	$(8.96 \pm 0.02) \times 10^6$	-39.66		
	308	$(8.77 \pm 0.02) \times 10^6$	-40.94	27.14	221.04
	318	$(8.41 \pm 0.01) \times 10^6$	-42.16		

value and that of the entropy changes can be obtained from the van't Hoff equation (Eq. 2):

$$\begin{aligned} \ln K_a &= -\Delta H^0/RT + \Delta S^0/R \\ \Delta G^0 &= \Delta H^0 - T\Delta S^0 \end{aligned} \quad (2)$$

Here, the associative binding constant, K_a , is the modified Stern–Volmer quenching constant at the corresponding temperature and R is the gas constant [22]. The results are presented in Table 1. The negative sign for the free energy (ΔG^0) means that the interaction process is spontaneous. In binary systems, the negative ΔH and positive ΔS indicated that electrostatic force played major roles for the acting force and the reaction was mainly enthalpy-driven. However, in the ternary system [(HSA–Aspirin)–Amlodipine], the positive ΔH^0 and ΔS^0 value is frequently taken as the reaction being mainly entropy-driven, with the enthalpy unfavorable for it, and with hydrophobic forces playing a major role. These results are confirmed by RLS results in previous work [14].

3.3 Time-Resolved Measurements

The fluorescence lifetime serves as a sensitive indicator of the local environment in which a given fluorophore is placed [23]. Lifetime measurements are rich in information and provide unique insights into the systems under investigation [24]. Fluorescence lifetime distributions originate from the existence of multiple conformational sub-states of the protein, and a distribution analysis of fluorescence decay data may provide information on the conformational landscape and enable detection of dynamics of the protein matrix on a picosecond/nanosecond time scale [25]. Mean (average) lifetimes $\langle t \rangle$ for biexponential decays of fluorescence were calculated from the decay times and pre-exponential factors using Eq. 3 [26]:

$$\langle \tau \rangle = \alpha_1 \tau_1 + \alpha_2 \tau_2 / \alpha_1 + \alpha_2 \quad (3)$$

where α is a pre-exponential factor representing the fractional contribution to the time-resolved decay of the component with a lifetime τ . Lifetime measurements of HSA were performed by exciting the sample at 290 nm in order to excite only the donor [27]. In HSA, such time-resolved fluorescence measurements have strongly suggested that the quenching is static in nature [28].

Fluorescence lifetime decay measurements supply one of the best parameters that help us to distinguish between static and dynamic processes.

It was of interest to study the fluorescence decay of the HSA protein at different molar ratios of the two drugs (Aspirin and Amlodipine) to obtain a picture of the change in the micro-environment of that fluorophore upon binding to the protein. Fluorescence lifetimes and their amplitudes are presented in Table 2. As shown, different values of τ were evidence that the various ligand concentrations had an effect on the protein. In order to further substantiate the quenching mechanism of the drugs to HSA, fluorescence lifetimes of HSA were ascertained in the absence and presence of Aspirin and Amlodipine. The decay curves fit well to a biexponential function and the relative fluorescence lifetime was $\tau = 3.67$ ns ($X^2 = 0.95$) for HSA. With addition of Aspirin, forming a binary system, the lifetime was $\tau = 3.22$ ns ($X^2 = 0.96$) and in the ternary system of (HSA–Amlodipine)–Aspirin, the lifetime was 3.15 ns ($X^2 = 0.96$). Also, at other conditions on addition of Amlodipine, the average fluorescence lifetime from a binary to a ternary system reduced the lifetime from 3.21 to 3.15 ns, attesting to the fact that the fluorescence quenching was essentially a static mechanism [24, 29]. In all systems, with the addition of the drug, the τ value of the natural protein was reduced. A reduction of about 3.2 was thus observed in both binary systems (HSA–Aspirin \approx HSA–Amlodipine). In the interaction of Amlodipine with HSA, the presence of the second drug reduced τ even further. The results thus show that in the presence of Aspirin, there was a greater bonding affinity of HSA–Amlodipine and this system was more static than the others. These results were also confirmed by the anisotropy studies.

3.4 Second-Derivative Fluorescence Spectroscopy

The second-derivative fluorescence spectroscopy technique enables characterization of even small changes in the local environment of Trp and Tyr (when excited at 280 nm). This is not obvious in conventional fluorescence spectra [30, 31], and can be attributed to the presence of Trp in various microenvironments with different hydrophobicity [32]. The techniques have increased the sensitivity of the

Table 2 Time-resolved fluorescence data of HSA in the absence and presence of Amlodipine and Aspirin in binary and ternary systems

System	τ_1 (ns)	α_1	τ_2 (ns)	α_2	τ (ns)	χ^2
HSA	1.927	0.6175	5.893	0.4864	3.671	0.9524
HSA–Aspirin	1.877	0.7514	5.859	0.3814	3.221	0.9619
(HSA–Amlodipine)–Aspirin	1.814	0.7327	5.813	0.3734	3.155	0.9673
HSA–Amlodipine	1.904	0.7663	5.841	0.3793	3.219	0.9539
(HSA–Aspirin)–Amlodipine	1.882	0.7625	5.802	0.3688	3.150	0.9644

basic absorption technique, thus making it possible to monitor small changes that take place in the environments of aromatic amino acids in proteins [33, 34]. These techniques become particularly useful in situations where large contributions of scattered light together with the attenuation of the signal (absorption or fluorescence) are studied. In this work, we have attempted to show that second-derivative fluorescence spectroscopy is a sensitive technique and that it takes place in the environments of aromatic amino acids (mainly Trp) in proteins [30].

Figure 2a shows the second-derivative fluorescence spectra of HSA and Amlodipine in the presence of Aspirin as a ternary system at pH 7.4. As can be seen, the negative band at 336 nm was the most sensitive to the changes in the ternary structure of HSA upon addition of Amlodipine in the presence of Aspirin. Minima at around 336 and 343 nm, a relatively fixed maximum at 381 nm and a

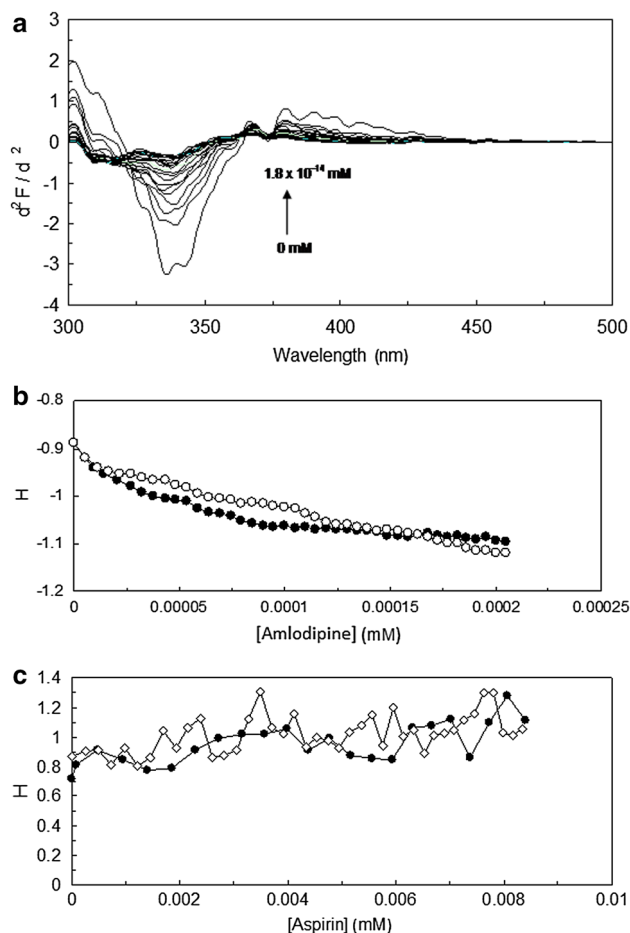


Fig. 2 a Second-derivative fluorescence spectra of HSA by adding various concentrations of Amlodipine in the presence of Aspirin at an excitation wavelength of 280 nm. Plots of parameter $H = h/h'$ versus concentration of Amlodipine (b) and c Aspirin as binary (open symbols) and ternary (filled symbols) systems. Conditions: $T = 298$ K, $\text{pH} = 7.4$, $\lambda_{\text{ex}} = 280$ nm, $[\text{HSA}] = 4.5 \times 10^{-3}$ mM, $[\text{Amlodipine}] = 0-1.8 \times 10^{-4}$ mM, $[\text{Aspirin}] = 0$ to 8.5×10^{-3} mM

shoulder at around 370 nm can be seen. As the concentration of Amlodipine was increased, the position and the intensity of the shortest wavelength band became altered, indicating a change in λ_{max} . Consequently, the micro-environment of Trp and Tyr changed more as the polarity was changed [35]. In addition, calculations of the value of H (which is indicative of the relative hydrophobicity of the Trp local environment) were performed from second-derivative spectra according to the method of Mozo-Villarias [30]. H is useful for monitoring average transitions taking place in Trp environments when proteins change their structure.

Figure 2b, c illustrates the obtained H factor as a function of the Amlodipine concentration for the HSA–Amlodipine complex and their ternary systems. From Fig. 2b H can be deduced that for the (HSA–Aspirin)–Amlodipine complex, fluorescence residues were in a more hydrophobic environment [31]. Similar effects appeared for HSA–Aspirin and (HSA–Amlodipine)–Aspirin, as shown in Fig. 2c. When the ionic strength was increased by addition of Aspirin, there was a substantial change in the second-derivative spectrum. The spectra for both ternary systems were typical of the highly hydrophobic environment. The complexes were formed in such a way that the Trp of the subunits was driven away from the solution [30].

The results were used to monitor apparent changes in these spectra when structural transitions were induced in the proteins and were associated with changes in the degree of polarity in the environments of all Trp in a protein. This indicates that in the presence of a second drug, the polarity around the Tyr residues was increased and the hydrophobicity was lowered. HSA has only one Trp residue in its sequence (position 214), in addition to 18 Tyr residues. This makes this protein useful for testing the influence of Tyr on second-derivative characteristics [9]. The different values of parameter H in binary and ternary systems suggest that Trp is in a more polar environment in the ternary system than in a binary system, which is in agreement with the fact that Trp 214 in a binary system is in a segment containing numerous charged residues.

3.5 Polydispersity Index (PI)

Techniques for the determination of molar mass and polydispersity are including mass spectrometry, laser light scattering, ultracentrifugation, electrophoresis and chromatography. Light-scattering measurements of polymer size are based on the observation that large particles scatter light very efficiently. In general, the ratio M_w/M_n is called the polydispersity index (or heterogeneity index). In this expression, M_w is the weight average molar mass and M_n is the number average molar mass. The term ‘monodisperse’ is conventionally applied to synthetic polymers in which

this index is less than 1.1. A collection of particles is usually polydisperse. It is therefore necessary to know not only the size of a certain particle, but also how many particles of the same size exist in the sample. Thus, we need an estimate of the size range present and the number or weight fraction of each particle size. A disperse system corresponds to the dispersion of small particles of one material in another. These small particles are commonly called colloids. In this context, small means less than about 500 nm is diameter (approximately the wavelength of light) [36].

The PI is an indication of the particle size distribution. The smaller the PI, the more consistent is the size distribution of dispersion. Depending on the polydispersity of the charge and the nature of the size dependence of the linear dissolution rate, the distribution may change in terms of the position of the median [37].

Figure 3a, b shows the polydispersity index (PI) versus the concentration of the drugs. A dispersion index of 0.1 indicates that the molecules forming the complex have structural similarities that are more homogeneous and in a more complex environment. A dispersion index of more than 0.1 means that the molecules have larger molecular masses and that they are diverse and heterogeneous. All of the complexes were considered to be polydisperse or

widely distributed since the polydispersity index was higher than 0.2. The dispersion index increased with an increasing drug concentration, which represents a distribution of heterogeneity in the environment.

For the HSA–Aspirin complex, when the concentration of Aspirin increased to about 0.006 mM, the PI remained constant. In (HSA–Amlodipine)–Aspirin, up to concentrations of about 0.004 mM, the dispersion increased after which it decreased. But in HSA–Amlodipine, for a concentration of about 0.0003 mM of Amlodipine, the PI value remained stable. The change in concentration thus had no effect on the polydispersity, and it was clear that HSA–Amlodipine produced the biggest particles that were also the most heterogeneous in size. It was observed that the PI values of the ternary systems (HSA–Aspirin)–Amlodipine and (HSA–Amlodipine)–Aspirin were close to 1 corresponding to a more heterogeneous solution, whereas for the binary systems of HSA–Amlodipine and HSA–Aspirin, the PI values were far from 1 and the solution was more homogeneous. For both binary systems (i.e., HSA–Amlodipine and HSA–Aspirin), the polydispersity index was lower than for the ternary systems. The presence of a second drug thus caused a decrease in the stability of the complexes. This suggests that increasing drug concentrations led to an increased heterogeneity of the solution, and the ternary systems were thus more heterogeneous than the binary systems.

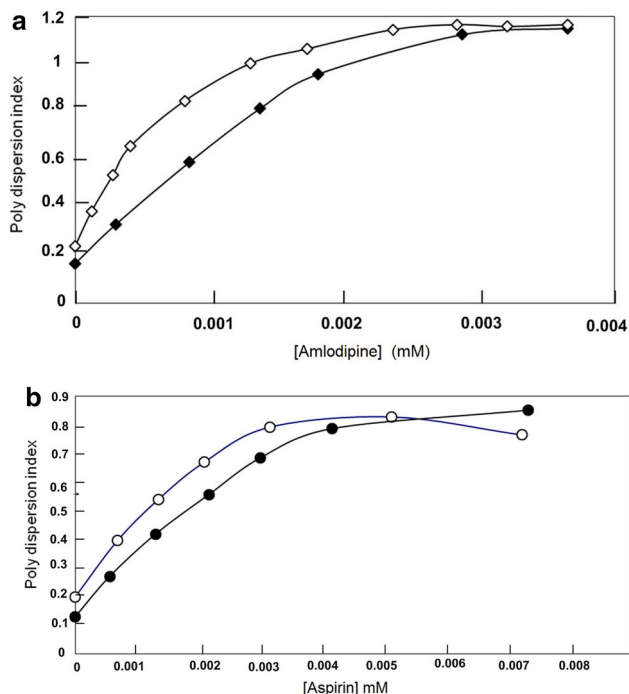


Fig. 3 Polydispersity data of HSA in the presence of Amlodipine (AML) (a) and Aspirin (ASA) (b) in binary (filled symbols) and ternary (open symbols) systems. Conditions: $T = 298$ K, $\text{pH} = 7.4$, $\lambda_{\text{ex}} = 280$ nm, $[\text{HSA}] = 4.5 \times 10^{-3}$ mM, $[\text{Amlodipine}] = 0$ – 1.8×10^{-4} mM, $[\text{Aspirin}] = 0$ to 8.5×10^{-3} mM

3.6 Mean Number and Zeta Potential Measurements

Many proteins are monodisperse, meaning that they have a single, definite molar mass [38]. A synthetic polymer, however, is polydisperse, in the sense that it comprises a mixture of molecules with various chain lengths and molar masses. The various techniques that are used to measure molar masses result in different types of mean values of polydisperse systems [36]. The potential located at the shear plane is known as the electrokinetic potential, or zeta potential. The zeta potential is the potential difference between the tightly bound layer (shear plane) and the electroneutral region of the solution. If the zeta potential is reduced below a certain value (which depends on the particular system being used), the attractive forces exceed their repulsive counterparts, and the particles come together [9]. As the protein conformation is already expanded at pH 7.4, drug/protein complexes might be formed as micelle-like clusters along the protein surface, in what may resemble the necklace model, with subsequent aggregation of these more hydrophobic complexes in order to avoid interaction with the solvent [39].

Dissolution of solid particles in a liquid medium is quite commonly encountered in the chemical process industry.

The equilibrium population between single drug/protein complexes and aggregated drug/protein complexes would be shifted to the latter. A previous report showed that when the Amlodipine concentration increased from 0 – 1.8×10^{-4} mM, the zeta potential shifted from a negative to a positive value [14]. A comparison between different systems shows that the highest concentration of Amlodipine and Aspirin led to the lowest points of maximum zeta potential. Also, this clearly took place in the ternary system in the presence of both drugs. It could thus be concluded that the presence of both drugs led to certain changes in the solution.

Dissolution changes particle diameters, causing the population of each size group to become altered and, in general, bringing about a change in the observed distribution of the number of particles as well as the volume or number versus particle size [40]. So, for a better analysis, Fig. 4a, b shows the effect of the Amlodipine and Aspirin concentrations on the size and number of particles in solution for the different complexes. In Fig. 4, it can be seen large shifts in the size distribution of the particle systems for the three different complexes. We also

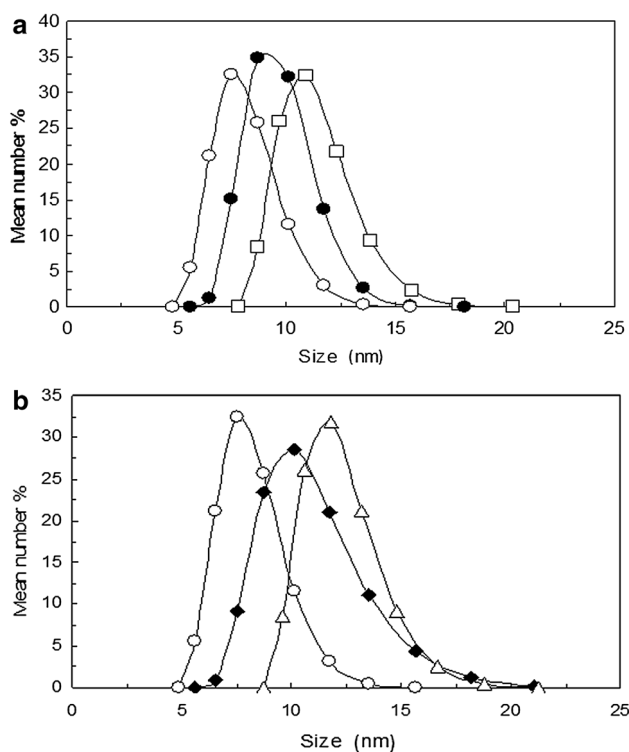


Fig. 4 Effects of the concentrations of Amlodipine (a) and Aspirin (b) on the size and number of HSA particles in solution (open circle); HSA–Amlodipine (filled circle); (HSA–Aspirin)–Amlodipine (open square) systems; HSA–Aspirin (filled diamond); (HSA–Amlodipine)–Aspirin (open triangle) systems. Conditions: $T = 298$ K, $\text{pH} = 7.4$, $\lambda_{\text{ex}} = 280$ nm, $[\text{HSA}] = 4.5 \times 10^{-3}$ mM, $[\text{Amlodipine}] = 0$ – 1.8×10^{-4} mM, $[\text{Aspirin}] = 0$ to 8.5×10^{-3} mM

observed that the size distribution for the ternary systems was higher than for the binary ones.

When comparing the systems, it was found that the size distribution of HSA in the presence of the first and second drug increased. Also, HSA–Amlodipine produced the biggest particles and had a larger polydispersion index in comparison with other complex solutions, whereas HSA–Aspirin gave rise to the smallest particles which were also the most homogeneous in size. The larger average particle size and the higher polydispersity index of Amlodipine indicated the presence of large aggregates of Amlodipine. This suggests a decrease in mean droplet size with an increasing drug concentration due to a larger interfacial area and a reduced interfacial tension [41, 42]. These results confirmed those from the PI measurements and what was observed for the HSA–Amlodipine complex: a large polydispersion index of the dispersions indicated a broad size distribution corresponding to changes in the micro-environment of the protein. This result was confirmed by RLS measurements [14].

3.7 Red Edge Excitation Shift (REES)

Red Edge Excitation Shift measurements are particularly useful for monitoring motions around the Trp residues in protein studies [43]. The REES is due to the electronic coupling between Trp indole rings and neighboring dipoles and occurs when there are slow relaxations of solvent media [44]. REES corresponds to a shift in the emission maximum toward a higher wavelength caused by a movement of the excitation wavelength toward the red edge of the absorption band [45]. The value of $\Delta\lambda_{\text{emmax}}$ is the difference in emission maxima when excited at 280 versus 295 nm [44]. Thus, in this study, we chose to excite the Trp at 280 and 295 nm to investigate the REES effect on the interaction between drugs and HSA. The results are listed in Table 3.

REES measurements upon interaction with Aspirin and Amlodipine as binary and ternary systems rendered it possible to compare the environmental and mobility features of the Trp residues in the HSA-drug complexes [46]. Moreover, the variability of the micro-environment of the protein occurred in the presence of drugs in all systems.

The value of $\Delta\lambda_{\text{emmax}}$ meant that the introduction of Aspirin and Amlodipine had an obvious impact on the mobility of the Trp micro-environment and that the Trp residue faced more restriction from its surroundings in the HSA-drug complexes. According to Table 3, the value of REES for the ternary system (HSA–Aspirin)–Amlodipine was about 7.0 nm, which indicated that the presence of Aspirin had an effect on the interaction between Amlodipine with HSA for a molar ratio 1:10 in comparison with the other complexes. By comparing the difference in

Table 3 The effect of Red Edge Excitation Shift (REES) for HSA with Aspirin and Amlodipine in binary and ternary systems at $\lambda_{\text{ex}} = 305$ nm and $\lambda_{\text{ex}} = 295$ nm, pH = 7.4, $T = 298$ K

System	Molar ratio (drug/HSA)	$\lambda_{280 \text{ nm}}$	$\lambda_{295 \text{ nm}}$	$\Delta\lambda$
HSA–Amlodipine	1:1	341	343	2
	1:5	339	342	3
	1:10	339	342	3
(HSA–Aspirin)–Amlodipine	1:1	338	341	3
	1:5	332	339	7
	1:10	330	337	7
HSA–Aspirin	1:1	339	343	4
	1:5	335	340	5
	1:10	333	338	5
(HSA–Amlodipine)–Aspirin	1:1	338	341	3
	1:5	336	340	4
	1:10	334	339	5

$\Delta\lambda_{\text{max}}$, it was observed that the tryptophan residue was irritable in the HSA–Amlodipine system. However, in the presence of Aspirin, the Trp micro-environment was more limited and permitted less movement. At this concentration of Amlodipine, a large complex was formed and there was a shift in the position of the emission maximum, reflecting changes in polarity around the Trp residue. On the other hand, the structure of the micro-environment of the Trp residue was altered and physiological functions of HSA were affected by Amlodipine.

3.8 Fluorescence Anisotropy

Fluorescence anisotropy is another type of observable fluorescence that can be very useful in molecular biophysics [47]. It is a powerful technique for investigating macromolecular dynamics, in which the sample is excited by linearly polarized light [48]. The fluorescence anisotropy is measured by first exciting a molecule with vertically polarized light, then observing the fluorescence intensity of emitted light passing through a polarizer held alternately parallel to and perpendicular to the direction of polarization of the incident light [49]. The instrument was set at configuration B, and the excitation and emission monochromators were set at the desired wavelengths. The cuvette was excited with vertically polarized light and the fluorescence intensity components I_{VV} and I_{VH} were alternately monitored (due to the L configuration of the instrument). Here, I_{VV} is the fluorescence intensity when both the excitation and emission polarizers are parallel and I_{VH} is the fluorescence intensity when the excitation and emission polarizers are perpendicular. The anisotropy (r) was calculated simultaneously by the instrument using Eq. 4:

$$r = I_{\text{VV}} - G \times I_{\text{VH}} / I_{\text{VV}} + 2 \times G \times I_{\text{VH}} \quad (4)$$

The G factor (which corrects the anisotropy introduced by the optical components of the detection system) was

obtained by the instrument before each anisotropy measurement where I_{VV} and I_{VH} are the vertically and horizontally polarized components of probe emission with excitation by vertically polarized light at the respective wavelength [50]. Measurements of the anisotropy (r) versus the protein concentration revealed the utility of the tautomer fluorescence anisotropy as a sensitive parameter for exploring structural changes in the protein.

Investigations of the fluorescence decay kinetics indicate heterogeneity in the microenvironments of the protein [51]. Slopes of lines fitted to experimental values determined, according to Eq. [2], the inverse of affinity constants ($1/K$). The K values were obtained for the ligands in the HSA solution without and with the competing drugs for two different concentrations. This can be seen in Fig. 5. The figure shows the fluorescence anisotropy of the drugs (Aspirin and Amlodipine) as a function of the HSA

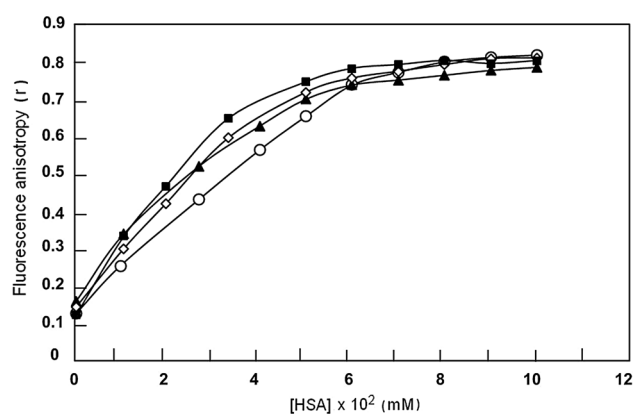


Fig. 5 Variation of the fluorescence anisotropy (r) of Amlodipine and Aspirin with the HSA concentration in binary [HSA–Amlodipine (filled triangle)]; [HSA–Aspirin (filled circle)]; and ternary [(HSA–Aspirin)–Amlodipine (filled square)]; [(HSA–Amlodipine)–Aspirin (open diamond)] systems. Conditions: $T = 298$ K, pH = 7.4, $\lambda_{\text{ex}} = 280$ nm, [HSA] = 4.5×10^{-3} mM, [Amlodipine] = $0-1.8 \times 10^{-4}$ mM, [Aspirin] = 0 to 8.5×10^{-3} mM

concentration as well as the changes in fluorescence anisotropy in the presence of the two competing drugs at varying concentration. The plot displays a marked increase in the fluorescence anisotropy of the fluorophore while moving from an aqueous environment to the HSA environment [52].

After the HSA concentration reached 10 μM , no significant increase in the binding of Aspirin and Amlodipine with HSA took place. The largest value of the fluorescence anisotropy was obtained when the drugs were present in the HSA–Amlodipine system, demonstrating that Amlodipine was bound to HSA. If the solution contained only free molecules of HSA, the anisotropy value would have been much lower. The anisotropy and K value of binding of HSA–Amlodipine decreased in the ternary form (HSA–Aspirin)–Amlodipine when going from 1.93×10^7 to $9.11 \times 10^6 \text{ M}^{-1}$ (data are not shown). Also when going from the binary (HSA–Aspirin) system to the ternary (HSA–Amlodipine)–Aspirin system, an increasing amount of proteins for various concentrations, decreased the steady-state value and the K values up to 1.08×10^6 to $4.71 \times 10^5 \text{ M}^{-1}$, respectively. The increase in anisotropy of Amlodipine and Aspirin bound HSA with an increase in protein concentration, indicating a reduction of the freedom of rotation of drugs bound to HSA. An increase in anisotropy could be due to a decreased Brownian motion or a lower energy transfer between identical chromophores [53]. The high anisotropy value ($r \approx 0.8$) found for (HSA–Aspirin)–Amlodipine suggests that, in the presence of Aspirin, Amlodipine bound at a site on HSA with motional restrictions.

The gradual increase in anisotropy of ligand emission with the HSA concentration is thus consistent with the picture that more and more ligand (Amlodipine and Aspirin) molecules become bound to HSA. The higher fluorescence anisotropy value associated with the drugs was due to its restricted motion as a result of its stabilizing electrostatic interaction in the binding site [51]. The anisotropy values suggest that both Aspirin and Amlodipine were rigidly bound in the protein.

3.9 Isothermal Titration Calorimetry (ITC)

Microcalorimetry is the measurement of the heat evolved or adsorbed by a chemical or physical process. Microcalorimetry has been used to study the interactions of drugs with food, lymphoma cells, microorganisms, blood, excipients, and cyclodextrin. One of the earliest uses of microcalorimetry was to investigate biological interactions of drugs [54]. The reasons for the widespread use of ITC for the determination of binding affinities are numerous and have been alluded to earlier [55]. It is the only analytical tool capable of directly measuring a thermodynamic

quantity and obviates the need for indirect determinations via van't Hoff analyses. In addition, careful experimental design renders it possible to determine further parameters from the same data set: the enthalpy ($\Delta_b H^0$) and entropy of binding ($\Delta_b S^0$), the Gibbs energy of binding ($\Delta_b G^0$) and the stoichiometry of binding (n).

The output from a conventional ITC experiment is a plot of power versus time, showing a series of peaks. These correspond to sequential injections of ligand solution into a substrate solution (Fig. 6, top). The integration of each peak results in a binding isothermal of enthalpy (kcal mol^{-1}) versus the molar ratio between ligand and substrate (Fig. 6, bottom). The binding isothermal is then fitted to a binding model, by least squares minimization, in order to derive the value of K_a (and, in the process, $\Delta_b H^0$) [56]. Figure 6a shows the ITC curve of the interaction of Amlodipine with HSA at 25 $^\circ\text{C}$. As shown, all peaks faced downward, indicating that the reactions were mainly exothermic [31]. They decreased progressively as unoccupied sites became saturated. The area of each peak is equal to the heat released per injection, which is proportional to the amount of the binding isothermal for the protein–ligand interaction in which the integrated heats (μJ) are plotted as a function of the molar ratio [57]. As shown, the analysis of the processed calorimetric curves suggests that the complex binary system is exothermic. The thermodynamic parameters for the interaction of Amlodipine and Aspirin with HSA, are summarized in Table 4. These enthalpies of binding of Amlodipine to HSA were more negative in the binary system as opposed to in its ternary counterpart. We determined the negative sign of the enthalpy changes as an eventual possibility that hydrophobic bonds may be formed during the interaction of Amlodipine with HSA [58].

Hydrophobic and weak electrostatic forces led to low values of K . Moreover, low affinity binding may be associated with conformational changes in the protein molecule [59]. So, according to Table 4, the value of K in the (HSA–Amlodipine)–Aspirin system was the lowest whereas it was higher in the HSA–Amlodipine system than in the other systems. On the other hand, the higher values of K for the HSA–Amlodipine system may also be due to the greater tendency of these molecules to self-associate [60, 61].

The changes in the entropy of binding ΔS^0 were largely caused by hydration effects: the entropy of hydration of polar and non-polar groups was thus large. The sign of ΔS^0 was negative and indicated that the binding process was dominated by hydrophobic interaction [58]. The value of ΔS^0 in the HSA–Amlodipine system was lower than in its ternary counterpart, indicating that protein molecules in this system underwent conformational changes in such a way that their flexibility increased [31]. In the presence of the second drug (Aspirin), upon drug association, the

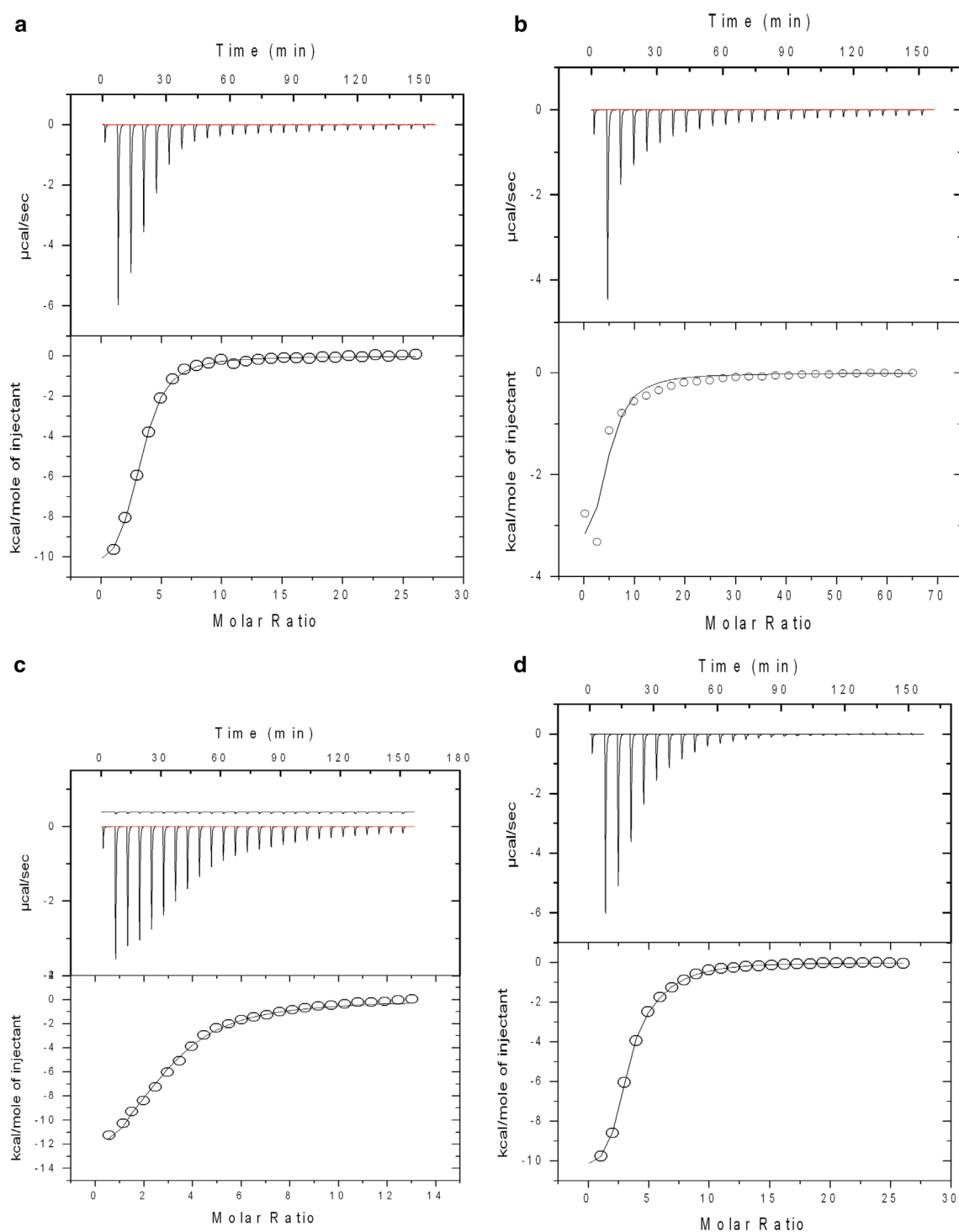


Fig. 6 Isothermal heat capacity curves for the binding of Amlodipine and Aspirin to HSA at 25 °C and pH 7.4. HSA–Amlodipine (a); (HSA–Aspirin)–Amlodipine (b) systems; HSA–Aspirin (c); (HSA–Amlodipine)–Aspirin (d) complex

entropy of interaction between Amlodipine and Aspirin with HSA decreased. However, ΔS^0 for the HSA–Aspirin system was $55.19 \text{ J mol}^{-1} \text{ K}^{-1}$ whereas it was $35.16 \text{ J mol}^{-1} \text{ K}^{-1}$ for the ternary (HSA–Amlodipine)–Aspirin system. This indicates that the interaction between Amlodipine and HSA in the ternary (HSA–Amlodipine)–

Aspirin system was more flexible than in the binary HSA–Aspirin system. Consequently, the presence of the second drug was important for the flexibility of the protein.

According to the views of Ross and Subramanian [62], positive ΔH^0 and ΔS^0 values are associated with hydrophobic interactions. Negative ΔH^0 and ΔS^0 values, on

Table 4 Thermodynamic characteristics of interaction of HSA with Amlodipine and Aspirin in binary and ternary systems according to ITC experiments at 25 °C

Systems	<i>n</i>	<i>K</i> (J mol ⁻¹)	ΔH^0 (kJ mol ⁻¹)	ΔS^0 (J mol ⁻¹ K ⁻¹)
HSA–Amlodipine	0.98	$(2.33 \pm 1.06) \times 10^7$	-21.11	68.02
(HSA–Aspirin)–Amlodipine	0.91	$(9.15 \pm 1.13) \times 10^6$	28.83	217.13
HSA–Aspirin	1.27	$(1.17 \pm 1.013) \times 10^6$	-17.79	55.19
(HSA–Amlodipine)–Aspirin	1.03	$(7.29 \pm 1.216) \times 10^5$	-20.19	35.16

the other hand, are associated with hydrogen bonding and Van der Waals forces. Finally, very low positive or negative ΔH^0 and positive ΔS^0 values are characteristic of electrostatic interactions. From Table 4, it can be seen that in all analyzed systems, the binding process was enthalpy-driven and the negative ΔH^0 values observed in the present study could not be attributed to electrostatic interactions. However, the binding became more enthalpy-driven with a favorable enthalpy and unfavorable entropy but in the ternary system of (HSA–Aspirin)–Amlodipine, the positive ΔH^0 and ΔS^0 values led to the presence of hydrophobic interactions and suggested that the process was entropy-driven. The large negative Gibbs energy for the drug binding may be due to the reduction in conformational freedom upon formation of coordinated bonds at the binding site [57, 62].

In conclusion, for the HSA–Amlodipine and HSA–Aspirin complexes, electrostatic interactions played the main roles but hydrophobic interactions could not be excluded. These results were confirmed by other techniques in this study. It can be suggested that the presence of the second drug (Aspirin) in the interaction of HSA–Amlodipine caused a specific interaction in comparison with other complexes.

3.10 Molecular Study

In our previous work [14], we have used molecular modeling techniques to study binary and ternary systems of drugs with HSA. According to the lowest number of K_i (inhibition constant) achieved from a docking study of HSA and two drugs, we could report that Aspirin was located in sub-domain IIA close to Lys199, while Amlodipine was located in a different site, the so-called site II, near Asp 255. We then analyzed the ternary docking system that was performed after energy minimization of the binary system of HSA plus each drug. The inhibitory constant was remarkably decreased after addition of Aspirin to the HSA–Amlodipine complex. Although each drug was located in a different position and had a non-competitive interaction, the affinity of each drug was affected by the other. It was assumed that since Aspirin and Amlodipine occupied different active sites they changed the secondary structure of HSA. In the binary systems, Lys199 for Aspirin and Asp 255, Asp 259 for Amlodipine,

were reported to be the most important residues in this regard. In the ternary (HSA–Aspirin)–Amlodipine system, Amlodipine was able to form a hydrogen bond with Glu311 but Aspirin did not show any hydrogen bonding in the ternary (HSA–Amlodipine)–Aspirin system.

3.10.1 Properties of Aspirin and Amlodipine

QSAR analyses of Aspirin and Amlodipine are summarized in Table 5. The more negative the hydration energy, the more stable was the molecule, and when comparing the results of the hydration energy of Amlodipine and Aspirin it was found that the Aspirin molecule was more stable than Amlodipine. This could be due to presence of amine and ester groups. The logarithm of partition coefficients ($\log P$) is useful for estimating the distribution of drugs within the body: hydrophobic molecules with high partition coefficients are preferentially distributed in hydrophobic compartments such as lipids, while hydrophilic drugs (with lower partition coefficients) are preferentially found in hydrophilic compartments such as blood serum.

The results of $\log P$ are in agreement with the results of hydration energy. Consequently, the value of $\log P$ in Amlodipine was higher than in Aspirin and the ability of Amlodipine to dissolve in the lipid phase was greater than that of Aspirin. It could also be concluded that Aspirin was more polar than Amlodipine, which caused more interactions with the hydrophilic regions of HSA. ProtScale diagrams showed about 11 highly hydrophobic sections in HSA at positions 10, 49, 98, 145, 198, 328, 349, 371, 482, 574 and 603. However, 21 major sections represented

Table 5 Quantitative structure activity relationship (QSAR) properties of Aspirin and Amlodipine as created by the HyperChem software

	Aspirin	Amlodipine
Log <i>P</i>	4.96	5.59
Surface area (grid) (<i>A</i> ²)	349.97	642.11
Volume (<i>A</i> ³)	535.60	1152.17
Hydration energy (Kcal/mol)	-10.98	-8.07
Refractivity (<i>A</i> ³)	17.39	64.89
Polarizability (<i>A</i> ³)	17.39	41.68
Mass (amu)	180.16	432.90
Partial charges (<i>e</i>)	0.0	0.0

hydrophilic properties at positions 24, 29, 38, 86, 118, 123, 127, 135, 159, 166, 213, 216, 360, 341, 419, 465, 469, 494, 545, 564 and 592 (Fig. 7). As displayed in Fig. 7, the bottom area of the hydrophobicity graph represents regions of HSA with lower hydrophobicity and higher hydrophilicity. A somehow similar method and diagram to the hydrophobicity diagram is the polarity diagram that takes into account which residues at position 84, 133, 212, 320, 547 and 585 that are highlighted and polar. Another interesting diagram extracted from ProtScale reveals exposed and accessible residues such as 218, 259, 295, 455 and 598. Since accessible residues are generally more polar than buried ones, the obtained graph agrees with the polarity graph. This condition provides a better situation for Amlodipine to interact with hydrophobic regions of HSA rather than Aspirin, but one should also consider that the large size of Amlodipine limits its interaction with buried residues of the protein.

Fig. 7 A ProtScale graph of human serum albumin (1A06). The *observed lines* represent the hydrophobicity and hydrophilicity profile from Kyte and Doolittle, accessible residues from Janin J. and polarity from Grantham R

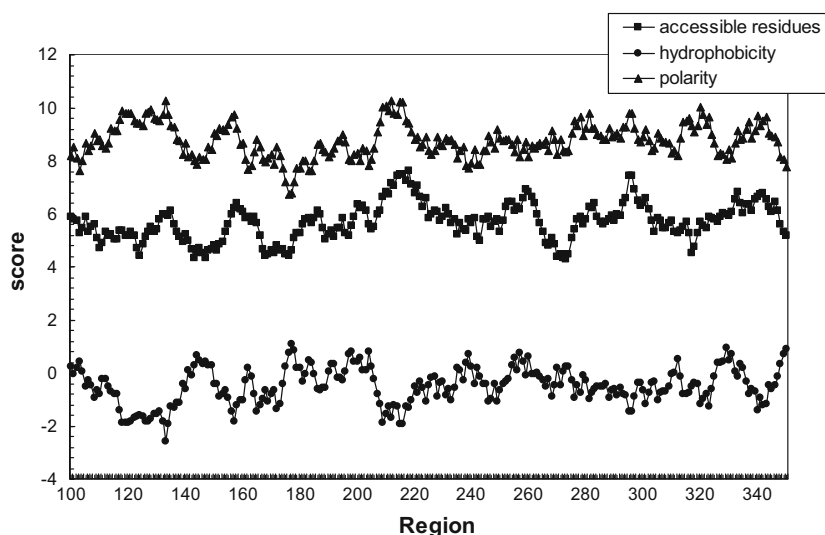


Fig. 8 Multiple sequence alignments generated by ClustalW (version 3 of the EBI software shows the most highly conserved residues in HSA). Conserved amino acid sequences are marked by *strings of ** on the second line of the sequence alignment

111	MADCCAKQEPERNECF LQHKDDNPN-LPRLV RPEVDVMCTAFHDNEETFLK KYLYEIARR	169	P02768
	: ** * *:: : . * . . :*: ::		
170	HPYFYAPEL LFFAKRYKAAFTECCQAADKAACL PKLDEL RDEGKAS SAKQR LKASLQK	229	P02768
	* : * : * : : . ** . * : :		
230	FGERAFKAWA--VARLSQRF PKAEFAEVSKLV DLT R VHT ECCHGDL LECADDRADLAKY	287	P02768
	.::: : : : : * : **.* : * .		
288	ICENQDSIS SKLKECCEK-P LLEKSHCIAEVENDEMPADLP SLAADFVESKDVCKNYAEA	346	P02768
	* *:		
347	KDVF LGMFLYEYAR--RHPD YSVV L LRLAKTYETT LEKCCAADPHECYA--KV FDE FK	402	P02768
	: : : : : . . : .		
403	PLVEEPQNLIRQNCLEFQ LGEYKFNALLVRYTKKVPQVSTPTLVEVSRNLGRVGSKCC	462	P02768
	. * : **: .*: . * : *		

In this study, we found conserved areas of HSA that can be candidates for drug molecule binding. For example, Cys occurred consistently in HSA more often than the other residues. It was observed in positions 124, 148, 192, 201, 268, 289, 303 and 313. Clearly, Cys is responsible for the disulfide bound in proteins and its consistency is probably affected by this. HSA is a heart-shaped protein with a deep valley and Cys could play a key role in its stability [63]. Another conserved residue is Pro 323, which again is an unusual amino acid that is not normally replaced by other amino acids due to its ring-shaped side-chain [11].

4 Conclusions

We have explored the binding of Amlodipine to HSA in the presence of Aspirin, as binary and ternary systems, in addition to the intrinsic fluorescence emission behavior of HSA. Time-resolved fluorescence measurements hint to the occurrence of static-type fluorescence quenching caused by specific interactions, mainly by ground-state complex formations. This is in agreement with the quenching obtained according to the Stern–Volmer relation. The present study also demonstrates that complexation between HSA with Amlodipine and Aspirin led to an increase in the steady-state fluorescence anisotropy. Binding of Amlodipine and Aspirin with HSA caused a dramatic enhancement of the fluorescence intensity and anisotropy (r), along with significant changes in the fluorescence excitation and emission profiles. Amlodipine also bound with higher affinity to binding sites on HSA as deduced by fluorescence anisotropy spectroscopy.

The results of zeta potential and RLS measurements rendered it possible to verify the existence of the interaction in the binding process. This modification is the first evidence of the existence of electrostatic interactions between the drug and protein, after the hydrophobic interaction is overcome. The polydispersity index and results from mean number measurements revealed that the presence of second drug caused a decrease in the stability of systems and increased the heterogeneity of complex.

A thermodynamic characterization enabled us to propose definitive conclusions regarding the energetic effect of protein–drug interactions and their correlation with the specificity of structural parameters of this protein. The negative values of enthalpy (ΔH^0) and entropy (ΔS^0) changes indicated that electrostatic interactions played major roles in stabilizing the complex. The thermodynamic parameters with regard to the binding of Amlodipine to HSA led us to believe that it was an enthalpy-controlled process. The multiple alignment results showed that sections around residues 100 through 300 were highly conserved. We were also able to confirm previously obtained

protein–ligand docking results, reported by our team with the results from this study. All residues involved in the interaction of Aspirin and Amlodipine with HSA as determined by the docking study were confirmed to be located in conserved areas that were even identical in some cases.

Finally, we concluded that the presence of Aspirin in (HSA–Aspirin)–Amlodipine system can cause a reduction in affinity of Amlodipine to binding in HSA. Whereas, in another system (HSA–Amlodipine)–Aspirin, at the Aspirin and Amlodipine beginning of binding has been affected with each other, subsequently interacted with HSA.

Acknowledgments The authors thank Dr. Ljungberg for the English editing.

Compliance with Ethical Standards

Funding The financial support of the Research Council of the Islamic Azad University–Mashhad Branch is gratefully acknowledged.

Conflict of interest The authors declare no conflicts of interest.

References

1. Kragh-Hansen U. Relations between high-affinity binding sites of markers for binding regions on human serum albumin. *Biochem J.* 1985;225(3):629–38.
2. Meti MD, Nandibewoor ST, Chimatadar SA. Binding studies of lincosamide antibiotic drug clindamycin phosphate to human serum albumin by fluorescence, 3D, and circular dichroism spectroscopy. *Montash Chem.* 2014;145(9):1519–27.
3. MacManus-Spencer LA, Tse ML, Hebert PC, Bischel HN, Luthy RG. Binding of perfluorocarboxylates to serum albumin: a comparison of analytical methods. *Anal Chem.* 2010;82(3):974–81.
4. Abdel-Wadood HM, Mohamed NA, Mahmoud AM. Validated spectrofluorometric methods for determination of amlodipine besylate in tablets. *Spectrochim Acta Part A Mol Biomol Spectrosc.* 2008;70(3):564–70.
5. Ni Y, Su S, Kokot S. Spectrofluorimetric studies on the binding of salicylic acid to bovine serum albumin using warfarin and ibuprofen as site markers with the aid of parallel factor analysis. *Anal Chim Acta.* 2006;580(2):206–15.
6. Warner TD, Mitchell JA. Cyclooxygenase-3 (COX-3): filling in the gaps toward a COX continuum? *Proc Natl Acad Sci USA.* 2002;99(21):13371–3.
7. Julian DG, Chamberlain DA, Pocock SJ. A comparison of aspirin and anticoagulation following thrombolysis for myocardial infarction (the AFTER study): a multicentre unblinded randomised clinical trial. *Br Med J.* 1996;313(7070):1429–31.
8. Vrettos JS, Meuse CW. Infrared techniques for quantifying protein structural stability. *Anal Biochem.* 2009;390(1):14–20.
9. Lakowicz JR. Principles of fluorescence spectroscopy. New York: Springer; 2006. pp. 1–954.
10. Bouchemal K. New challenges for pharmaceutical formulations and drug delivery systems characterization using isothermal titration calorimetry. *Drug Discovery Today.* 2008;13(21–22):960–72.

11. Twyman R. Principles of proteomics. Garland: Garland Science; 2013.
12. Cai L, Tao X, Liu Y, Zhang H, Gao L, Hu S, et al. Molecular characteristics and phylogenetic analysis of N gene of human derived rabies virus. *Biomed Environ Sci*. 2011;24(4):431–7.
13. Walker JM. The proteomics protocols handbook. Berlin: Springer; 2005.
14. Abdollahpour N, Asoodeh A, Saberi MR, Chamani J. Separate and simultaneous binding effects of aspirin and amlodipine to human serum albumin based on fluorescence spectroscopic and molecular modeling characterizations: a mechanistic insight for determining usage drugs doses. *J Lumin*. 2011;131(9):1885–99.
15. Apweiler R, Bateman A, Martin MJ, O'Donovan C, Magrane M, Alam-Faruque Y, et al. Activities at the Universal Protein Resource (UniProt). *Nucleic Acids Res*. 2014;42(D1):D191–8.
16. Ooi T, Oobatake M, Némethy G, Scheraga HA. Accessible surface areas as a measure of the thermodynamic parameters of hydration of peptides. *Proc Natl Acad Sci USA*. 1987;84(10):3086–90.
17. Ghose AK, Crippen GM. Atomic physicochemical parameters for three-dimensional-structure-directed quantitative structure-activity relationships. 2. Modeling dispersive and hydrophobic interactions. *J Chem Inf Comput Sci*. 1987;27:21–35.
18. Bojko B, Sułkowska A, Maciazek M, Równicka J, Njau F, Sułkowski WW. Changes of serum albumin affinity for aspirin induced by fatty acid. *Int J Biol Macromol*. 2008;42(4):314–23.
19. Amani N, Saberi MR, Chamani JK. Investigation by fluorescence spectroscopy, resonance rayleigh scattering and zeta potential approaches of the separate and simultaneous binding effect of paclitaxel and estradiol with human serum albumin. *Protein Pept Lett*. 2011;18(9):935–51.
20. Hu X, Cui S, Liu JQ. Fluorescence studies of interaction between flavonol p-coumaroylglucoside tiliroside and bovine serum albumin. *Spectrochim Acta Part A Mol Biomol Spectrosc*. 2010;77(2):548–53.
21. Wang T, Xiang BR, Li Y, Chen CY, Zhou XH, Wang ZM, et al. Studies on the binding of a carditonic agent to human serum albumin by two-dimensional correlation fluorescence spectroscopy and molecular modeling. *J Mol Struct*. 2009;921(1–3):188–98.
22. Yq Wang, Bp Tang, Hm Zhang, Zhou Qh, Gc Zhang. Studies on the interaction between imidacloprid and human serum albumin: spectroscopic approach. *J Photochem Photobiol B*. 2009;94(3):183–90.
23. Maciejewski A, Demmer DR, James DR, Safarzadeh-Amiri A, Verrall RE, Steer RP. Relaxation of the second excited singlet states of aromatic thiones: the role of specific solute-solvent interactions. *J Am Chem Soc*. 1985;107(10):2831–7.
24. Bright FV, Munson CA. Time-resolved fluorescence spectroscopy for illuminating complex systems. *Anal Chim Acta*. 2003;500(1–2):71–104.
25. Ferreira ST, Stella L, Gratton E. Conformational dynamics of bovine Cu, Zn superoxide dismutase revealed by time-resolved fluorescence spectroscopy of the single tyrosine residue. *Biophys J*. 1994;66(4):1185–96.
26. Shannigrahi M, Bagchi S. Dual probe solubilisation in two distinct regions of pure and mixed micelles: a pico-second time resolved fluorescence study. *Chem Phys Lett*. 2004;396(4–6):367–71.
27. Banerjee P, Ghosh S, Sarkar A, Bhattacharya SC. Fluorescence resonance energy transfer: a promising tool for investigation of the interaction between 1-anthraccene sulphionate and serum albumins. *J Lumin*. 2011;131(2):316–21.
28. Mandal P, Bardhan M, Ganguly T. A detailed spectroscopic study on the interaction of Rhodamine 6G with human hemoglobin. *J Photochem Photobiol B*. 2010;99(2):78–86.
29. Chakrabarty A, Mallick A, Haldar B, Purkayastha P, Das P, Chattopadhyay N. Surfactant chain-length-dependent modulation of the tropotropic transformation of a biological photosensitizer: Norharmane in anionic micelles. *Langmuir*. 2007;23(9):4842–8.
30. Mozo-Villariás A. Second derivative fluorescence spectroscopy of tryptophan in proteins. *J Biochem Biophys Methods*. 2002;50(2–3):163–78.
31. Chamani J, Vahedian-Movahed H, Saberi MR. Lomefloxacin promotes the interaction between human serum albumin and transferrin: a mechanistic insight into the emergence of antibiotic's side effects. *J Pharm Biomed Anal*. 2011;55(1):114–24.
32. Kumar V, Sharma VK, Kalonia DS. Second derivative tryptophan fluorescence spectroscopy as a tool to characterize partially unfolded intermediates of proteins. *Int J Pharm*. 2005;294(1–2):193–9.
33. Padrós E, Duñach M, Morros A, Sabés M, Mañosa J. Fourth-derivative spectrophotometry of proteins. *Trends Biochem Sci*. 1984;9(12):508–10.
34. Mozo-Villariás A, Morros A, Andreu JM. Thermal transitions in the structure of tubulin - Environments of aromatic aminoacids. *Eur Biophys J*. 1991;19(6):295–300.
35. Sarzehi S, Chamani J. Investigation on the interaction between tamoxifen and human holo-transferrin: determination of the binding mechanism by fluorescence quenching, resonance light scattering and circular dichroism methods. *Int J Biol Macromol*. 2010;47(4):558–69.
36. Atkins P, De Paula J. Elements of physical chemistry. Oxford: Oxford University Press; 2012.
37. Bhattacharya A. Predicting rates of dissolution of polydisperse solids in reactive media. *Chem Eng Process*. 2007;46(6):573–83.
38. Privalov P. Proteins which do not present a single cooperative system. *Adv Protein Chem*. 1982;35:1–104.
39. Cheema MA, Taboada P, Barbosa S, Gutiérrez-Pichel M, Castro E, Siddiq M, et al. Energetics of binding and protein unfolding upon amphiphilic drug complexation with a globular protein in different aqueous media. *Colloids Surf B*. 2008;63(2):217–28.
40. Subramanian B, Kuo F, Ada E, Kotyla T, Wilson T, Yoganathan S, et al. Enhancement of anti-inflammatory property of aspirin in mice by a nano-emulsion preparation. *Int Immunopharmacol*. 2008;8(11):1533–9.
41. Peng LC, Liu CH, Kwan CC, Huang KF. Optimization of water-in-oil nanoemulsions by mixed surfactants. *Colloids Surf A*. 2010;370(1–3):136–42.
42. Liu CH, Yu SY. Cationic nanoemulsions as non-viral vectors for plasmid DNA delivery. *Colloids Surf B*. 2010;79(2):509–15.
43. Klajnert B, Stanisławska L, Bryszewska M, Pałecz B. Interactions between PAMAM dendrimers and bovine serum albumin. *Biochim Biophys Acta Proteins Proteom*. 2003;1648(1–2):115–26.
44. Zhang HM, Wang YQ, Jiang ML. A fluorimetric study of the interaction of C.I. Solvent Red 24 with haemoglobin. *Dyes Pigments*. 2009;82(2):156–63.
45. Shang L, Wang Y, Jiang J, Dong S. pH-dependent protein conformational changes in albumin: gold nanoparticle bioconjugates: a spectroscopic study. *Langmuir*. 2007;23(5):2714–21.
46. Omidvar Z, Parivar K, Saneh H, Amiri-Tehranizadeh Z, Baratian A, Saberi MR, et al. Investigations with spectroscopy, zeta potential and molecular modeling of the non-cooperative behaviour between cyclophosphamide hydrochloride and aspirin upon interaction with human serum albumin: binary and ternary systems from the view point of multi-drug therapy. *J Biomol Struct Dyn*. 2011;29(1):181–206.
47. Royer CA. Approaches to teaching fluorescence spectroscopy. *Biophys J*. 1995;68(3):1191–5.
48. Bensikaddour H, Snoussi K, Lins L, Van Bambeke F, Tulkens PM, Brasseur R, et al. Interactions of ciprofloxacin with DPPC

- and DPPG: fluorescence anisotropy, ATR-FTIR and ³¹P NMR spectroscopies and conformational analysis. *Biochim Biophys Acta Biomembr.* 2008;1778(11):2535–43.
49. Anderson CO, Niesen JFM, Blanch HW, Prausnitz JM. Interactions of proteins in aqueous electrolyte solutions from fluorescence anisotropy and circular-dichroism measurements. *Biophys Chem.* 2000;84(2):177–88.
 50. Sanz-Vicente I, Castillo JR, Galbán J. Fluorescence anisotropy: application in quantitative enzymatic determinations. *Talanta.* 2005;65(4):946–53.
 51. Chaudhuri S, Pahari B, Sengupta PK. Ground and excited state proton transfer and antioxidant activity of 7-hydroxyflavone in model membranes: absorption and fluorescence spectroscopic studies. *Biophys Chem.* 2009;139(1):29–36.
 52. Wybranowski T, Cyrankiewicz M, Ziolkowska B, Kruszewski S. The HSA affinity of warfarin and flurbiprofen determined by fluorescence anisotropy measurements of camptothecin. *BioSystems.* 2008;94(3):258–62.
 53. Li Y, He W, Liu H, Yao X, Hu Z. Daidzein interaction with human serum albumin studied using optical spectroscopy and molecular modeling methods. *J Mol Struct.* 2007;831(1–3):144–50.
 54. Koenigbauer MJ. Pharmaceutical applications of microcalorimetry. *Pharm Res.* 1994;11(6):777–83.
 55. Miller KR, Cistola DP. Titration calorimetry as a binding assay for lipid-binding proteins. *Mol Cell Biochem.* 1993;123(1–2):29–37.
 56. Gaisford S, O'Neill MAA. *Pharmaceutical isothermal calorimetry.* London: Informa Healthcare; 2006.
 57. Griko YV, Remeta DP. Energetics of solvent and ligand-induced conformational changes in α -lactalbumin. *Protein Sci.* 1999;8(3):554–61.
 58. Dimitrova MN, Matsumura H, Terezova N, Neytchev V. Binding of globular proteins to lipid membranes studied by isothermal titration calorimetry and fluorescence. *Colloids Surf B.* 2002;24(1):53–61.
 59. Haberland ME, Reynolds JA. Interaction of L α palmitoyl lysophosphatidylcholine with the AI polypeptide of high density lipoprotein. *J Biol Chem.* 1975;250(17):6636–9.
 60. Lovrien R, Sturtevant JM. Calorimetric determination of the enthalpies of binding of ions to deionized bovine serum albumin. *Biochemistry.* 1971;10(21):3811–5.
 61. Banerjee SK, Pogolotti A Jr, Rupley JA. Self association of lysozyme. Thermochemical measurements: effect of chemical modification of TRP 62, TRP 108, and GLU 35. *J Biol Chem.* 1975;250(20):8260–6.
 62. Ross PD, Subramanian S. Thermodynamics of protein association reactions: forces contributing to stability. *Biochemistry.* 1981;20(11):3096–102.
 63. Grantham R. Amino acid difference formula to help explain protein evolution. *Science.* 1974;185(4154):862–4.